[Article ID] 1003- 6326(2001)02- 0183- 05

Electrode characteristics of non-stoichiometric Ml(NiMnAlFe)$_x$ alloys①

ZHANG Shu-kai(张书凯)[1], LEI Yong-quan(雷永泉)[1], CHEN Li-xin(陈立新)[1],
SHU Kang-ying(舒康颖)[1], ZHANG Yao(张 耀)[1], WANG Qi-dong(王启东)[1], LÜ Guang-lie(吕光烈)[2]
(1. Department of Materials Science and Engineering, Zhejiang University,
Hangzhou 310027, P. R. China;
2. Central Laboratory, Zhejiang University, Hangzhou 310028, P. R. China)

[Abstract] The phase structure and electrochemical properties of Co-free Ml($Ni_{0.82}Mn_{0.07}Al_{0.06}Fe_{0.05}$)$_x$ alloys with stoichiometry $4.6 \leqslant x \leqslant 5.6$ were investigated. The results revealed that most of the as-cast non-stoichiometric alloys have the main $CaCu_5$ type structure with a small amount of La_2Ni_7 and LaNi or AlNi secondary phase, the alloys all have typical dendrite structure, the lattice parameter of the alloys increases with the decrease of stoichiometry. Electrochemical measurements showed that the stoichiometric alloy $AB_{5.0}$ (the Ml($Ni_{0.82}Mn_{0.07}Al_{0.06}Fe_{0.05}$)$_x$ alloy with $x = 5.0$) has the highest discharge capacity (310 mAh·g^{-1}), and the over-stoichiometric alloys have relatively higher cycling stability and high-rate dischargeability than others although their maximum discharge capacities are relatively lower compared with the $AB_{5.0}$ alloy.

[Key words] hydrogen storage alloys; non-stoichiometry; phase structure; electrochemical properties
[CLC number] TG 132 [Document code] A

1 INTRODUCTION

Mischmetal based AB_5-type Mm(NiCoMnAl)$_5$ alloys are now widely used as the negative electrode materials of Ni/MH batteries. Among the elements of the alloys, Co has been believed to have the effect of lowering the volume expansion of the compound on hydrogenation[1] and preventing the alloying element Mn to dissolve into the KOH solution[2], and thereby was believed to improve the electrochemical cycling stability of the alloys. However, because Co is the most expensive materials in the alloy, in order to decrease the alloy cost, it is necessary to find some low-cost elements to replace Co without deteriorating the cycling stability property and other electrochemical properties of the alloys. In resent years, several Co-free or low-Co alloys containing Cu, Si, Cr etc have been developed[3~6], and Fe has been proven to have an important effect on increasing the cycling stability of some low-Co alloys too[7,8]. However, these Co-free or low-Co alloys generally have a shorter cycle life compared with the high-Co (10%) alloys.

It is also known that the stoichiometry of the alloys significantly affects the electrochemical properties. Notten and his co-workers studied La(NiCu)$_x$ alloys and found that the cycling stability noticeably increased with the increase of stoichiometry x in the range of $5 < x < 6$, but the maximum discharge capacity of the alloys decreased at the same time[9,10]. Higashiyama and his co-workers studied the low-Co Mm($Ni_{3.8}Al_{0.2}Mn_{0.6}$)$_{(x-0.4)/4.6}Co_{0.4}$ alloys, and found that the cycling stability is improved at $x = 5.2$ and $x = 5.4$, and the discharge capacity lowered with the increase of stoichiometry within $5.0 < x < 5.8$[11]. So far, no detailed information on the effect of stoichiometry on Co-free Fe-containing alloy is available in the references.

In this work, the element Fe is selected to replace Co, and the effects of non-stoichiometry on the electrochemical properties of Co-free alloys Ml(NiMnAlFe)$_x$ ($4.6 \leqslant x \leqslant 5.6$) as active electrode materials were investigated.

2 EXPERIMENTAL

Ml($Ni_{0.82}Mn_{0.07}Al_{0.06}Fe_{0.05}$)$_x$ ($4.6 \leqslant x \leqslant 5.6$) alloy samples were prepared by arc melting in argon atmosphere and remelted three times to ensure higher homogeneity. Ml stands for La-rich mischmetal with the composition of 54.7% La, 29.5% Ce, 12.0% Pr, 3.5% Nd and 0.3% impurity, and all other starting elemental metals have a purity higher than 99.9%.

The alloy samples were ground mechanically into powders (< 50 μm) and used for both electrochemical measurements and X-ray diffraction (XRD) analysis. For the electrochemical measurements the alloy powder (about 100 mg) was mixed with electrolytic copper powder (44 μm) in a mass ratio of 1∶2 and cold pressed to a electrode pellets (d = 10 mm). Electrochemical measurements were carried out at 25 ℃ in a tri-electrode half cell with Ni(OH)$_2$/NiOOH as the counter electrode and Hg/HgO as the reference elec-

① [Foundation item] Project 863- 715- 004- 0060 supported by National Advanced Materials Committee of China
[Received date] 2000- 05- 11; [Accepted date] 2000- 10- 08

trode, in a 6 mol/L KOH electrolyte. The electrode activation and maximum capacity C_{max} were measured at the charge-discharge current of 50 $mA \cdot g^{-1}$ until discharged to − 0.6 V (vs Hg/HgO). The high-rate dischargeability (%), defined as $C_n \times 100/(C_n + C_{50})$, was determined from the ratio of the discharge capacity C_n at n= 300, 600 or 900 $mA \cdot g^{-1}$ to the total discharge capacity defined as the sum of C_n and C_{50}, the additional capacity measured subsequently at 50 $mA \cdot g^{-1}$. The cycling test was conducted at the charge-discharge current of 300 $mA \cdot g^{-1}$. The cycling capacity retention rate S_{300} and S_{500} were defined as $S_{300}(\%) = C_{300th} \times 100/C_{max}$ and $S_{500} = C_{500th} \times 100/C_{max}$, where C_{300th} and C_{500th} are the discharge capacity at the 300th and 500th cycle respectively.

The phase structure of the samples was determined by XRD analysis by using an X-ray diffractometer of Rikagu D/Max-313 with CuK_α radiation. The microstructure and the composition of the samples were examined by using a scanning electron microscope (SEM) Philips-XL30 and EDS.

3 RESULTS AND DISCUSSION

Fig. 1 shows the XRD patterns of the $Ml(Ni_{0.82}Mn_{0.07}Al_{0.06}Fe_{0.05})_x$ ($4.6 \leqslant x \leqslant 5.6$) alloys. It can be seen that most of these alloys are indexed to have a main phase with $CaCu_5$ type structure and a few secondary phases. The secondary phases are identified to be La_2Ni_7 and LaNi for the alloys with $x \leqslant 5.0$, while that for $x > 5.0$ is AlNi. From Fig. 1 it can also be seen that the peaks of secondary phases La_2Ni_7 and LaNi get higher when x decreases in the range of $4.6 \leqslant x \leqslant 5.0$, and that of AlNi become lower in the range of $5.2 \leqslant x \leqslant 5.6$.

The lattice parameters and Rietveld analysis results of the $Ml(Ni_{0.82}Mn_{0.07}Al_{0.06}Fe_{0.05})_x$ ($4.6 \leqslant x \leqslant 5.6$) alloys are listed in Table 1. It can be seen that the amount of secondary phases La_2Ni_7 and LaNi increases when x decreases from 5.0 to 4.6, and that of the secondary phase AlNi increases when x increases from 5.2 to 5.6. Besides the $CaCu_5$ main

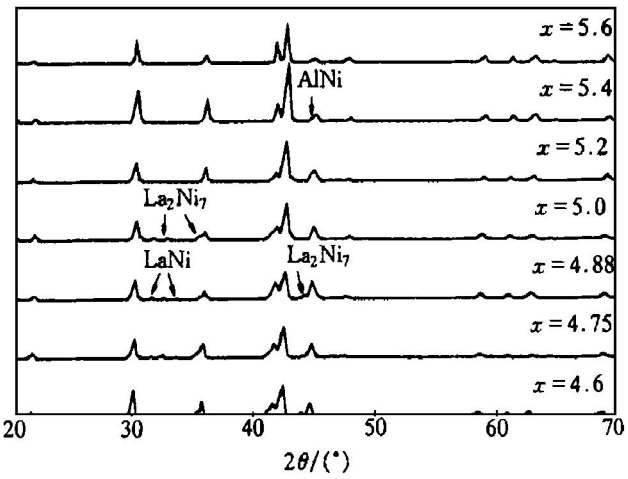

Fig. 1 XRD patterns of alloys $Ml(Ni_{0.82}Mn_{0.07}Al_{0.06}Fe_{0.05})_x$ ($4.6 \leqslant x \leqslant 5.6$)

phase, the alloy $AB_{4.6}$ has 21.8% La_2Ni_7 and 3.85% LaNi phases, the $AB_{5.0}$ alloy has 4.6% La_2Ni_7 and 0.6% LaNi phases, while the $AB_{5.6}$ alloy has 0.6% AlNi phase. The lattice parameters all decrease with the increase of the stoichiometry x except for x = 5.6. From Table 1 it can be also seen that the crystalline size of the alloys is changed due to the different stoichiometry. The crystalline sizes in a-axis and b-axis increase with the increase of stoichiometry, while the crystalline size in c-axis decreases with the increase of stoichiometry.

It was suggested by Notten[9, 10] that when stoichiometry x was less than 5.0, a part of A-elements, i.e., rare-earth elements, in the alloys have to occupy B-side sites. This leads to a pronounced increase in the lattice constants. On the other hand, when $x > 5.0$, part of B-elements i.e., Ni, Mn, Al and Fe, in the over-stoichiometric alloys have to occupy A-side sites, leading to a decrease in the lattice constant. But at x = 5.6, it can be seen that the lattice parameters c is larger than that of x = 5.2 and 5.4. There could be two reasons for it. Firstly, there are some secondary phase (AlNi) in the alloy $AB_{5.6}$ (Fig. 2), whose appearance makes the main phase become very close to that of stoichiometric AB_5. Se-

Table 1 Phase abundance, lattice parameters and crystalline sizes of alloys $Ml(Ni_{0.82}Mn_{0.07}Al_{0.06}Fe_{0.05})_x$ ($4.6 \leqslant x \leqslant 5.6$)

Stoichiometry (x)	Phase abundance				Crystalline size/nm		Lattice constants		
	$LaNi_5$	La_2Ni_7	LaNi	AlNi	$M_{11,22}$	M_{33}	a/nm	c/nm	V/nm^3
4.6	74.4	21.8	3.6	–	11.16	35.18	0.501 67	0.406 71	0.088 64
4.75	75.7	22.3	2.0	–	57.90	31.23	0.501 57	0.406 71	0.088 61
4.88	81.1	16.6	2.3	–	57.19	25.58	0.501 56	0.405 55	0.088 35
5.0	94.6	4.8	0.6		58.64	26.79	0.501 28	0.405 58	0.088 26
5.2	99.7	–	–	0.3	66.74	27.78	0.500 96	0.405 12	0.088 05
5.4	99.6	–	–	0.4	82.06	27.60	0.500 55	0.404 79	0.087 83
5.6	99.4	–	–	0.6	142.18	22.56	0.500 53	0.405 15	0.087 90

Note: $M_{11,22}$ is crystalline size in a-axis and b-axis, M_{33} is crystalline size in c-axis direction

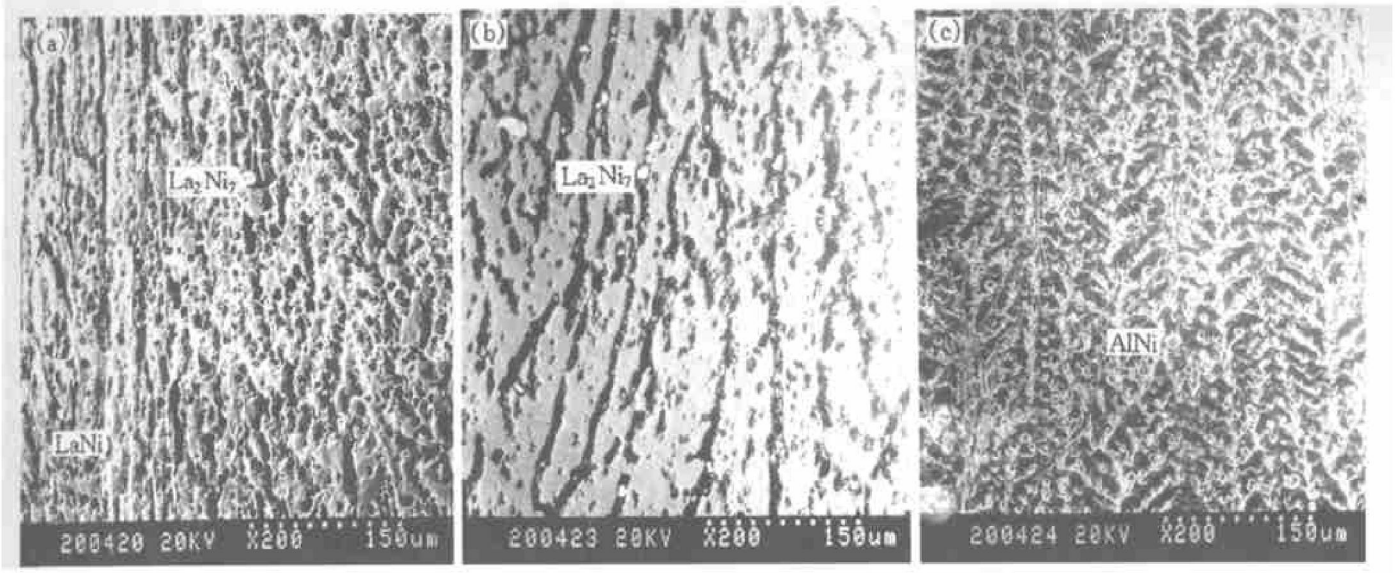

Fig. 2 SEM microstructures of alloys Ml$(Ni_{0.82}Mn_{0.07}Al_{0.06}Fe_{0.05})_x$
(a) —x = 4.6; (b) —x = 5.0; (c) —x = 5.4

condly, with the increase of stoichiometry x, the B-side atoms with small atom radii increase, the probability of two B atoms to occupy one A site increases, which makes the lattice constant increase. It has been reported that if A-side atoms are replaced by dumbbell pairs of B-type atoms in MmB_5 alloys, the lattice parameter a will decrease, and c will increase[9,10], this is in agreement with our results.

Fig. 2 shows the microstructures of the alloys $AB_{4.6}$, $AB_{5.0}$ and $AB_{5.4}$. All these alloys have coarse dendrite structure with the presence of some secondary phases. By EDS analysis, the trunk, arm and the region between arms of the dendrite are all $CaCu_5$ type structure phase with slightly different compositions. The secondary phases which mainly in the region between arms of the dendrite are LaNi, La_2Ni_7 or AlNi with other elements in it. This is in agreement with the result of XRD.

The activation process and maximum discharge capacities of the alloys Ml$(NiMnAlFe)_x$ (x = 4.6, 5, 5.4) are shown in Fig. 3. The reversible capacity of the system AB_x is the maximum for the stoichiometric alloy Ml$(NiMnAlFe)_5$ (C_{max} = 310.5 mAh·g^{-1}). The capacity of non-stoichiometric alloys is all lower to different extent. The activation properties of these alloys are also different. The stoichiometric alloy (x = 5.0) and over-stoichiometric alloys ($x > 5.0$) have good activation property, they need 4~5 cycles to reach their maximum capacity. The activation process of under-stoichiometric alloys ($x < 5.0$) is relatively more difficult and it takes about 7 cycles to reach its highest discharge capacity for x = 4.75. Because of the presence of secondary phase La_2Ni_7 and LaNi in $x \leqslant 5.0$, and that of AlNi in $x > 5.0$, the total amount of hydrogen storage phase ($CaCu_5$ structure phase) decreases with the increase of the secondary phases. It has been reported that the hydride of La_2Ni_7 and

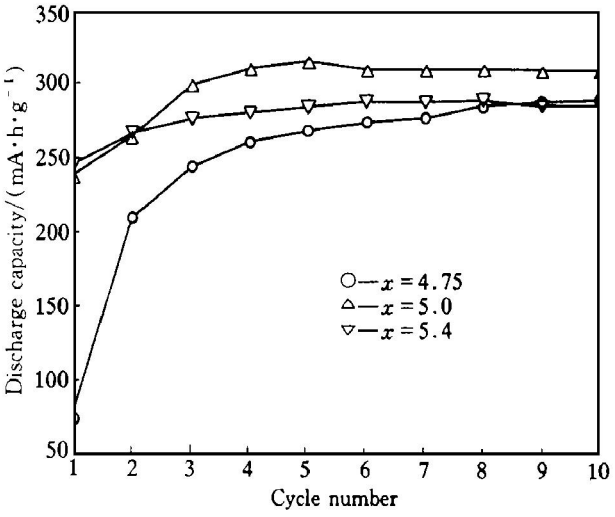

Fig. 3 Initial activation process of Ml$(Ni_{0.82}Mn_{0.07}Al_{0.06}Fe_{0.05})_x$

LaNi is so stable in the charge-discharge cycling that its discharge capacity approaches zero[12], while the AlNi phase does not store hydrogen at all. For this reason capacity of the alloys decrease with the appearance of these secondary phases. At the same time, the discharge capacity decreases also due to the decrease of cell volume for the over-stoichiometric alloys.

From Fig. 4 and Table 2, it can be seen that over-stoichiometric alloys have a better cycle life than the stoichiometric alloy $AB_{5.0}$. After 300 charge-dischargecycles, the capacity attenuation rate (S_{300}) of $AB_{4.6}$ is 79.1%, and those of the $AB_{5.0}$ and $AB_{5.4}$ are 66.0% and 67.5%, respectively. But for increased number of cyclings, the cycling stability is different somewhat. The over-stoichiometric alloys show much better cycling stability compared with that of the alloys with $x \leqslant 5.0$ at high cycling num-

Table 2 Electrochemical properties of alloys $Ml(Ni_{0.82}Mn_{0.07}Al_{0.06}Fe_{0.05})_x$ ($4.6 \leqslant x \leqslant 5.6$)

Stoichometry (x)	Discharge capacity /(mAh·g^{-1})	Cycling stability /%		High-rate dischargeability(%) at different discharge current density/(mA·g^{-1})		
		S_{300}	S_{500}	300	600	900
4.6	274.3	79.1	30.3	84.7	60.2	40.1
4.75	279.6	68.3		78.2	65.8	52.5
4.88	296.0	61.5		87.9	73.7	62.4
5.0	310.5	66.0	45.1	87.2	74.2	62.5
5.2	305.8	57.9		80.6	68.1	64.3
5.4	289.2	67.5	48.9	78.9	71.6	66.6
5.6	284.3	61.9		83.2	83.2	83.1

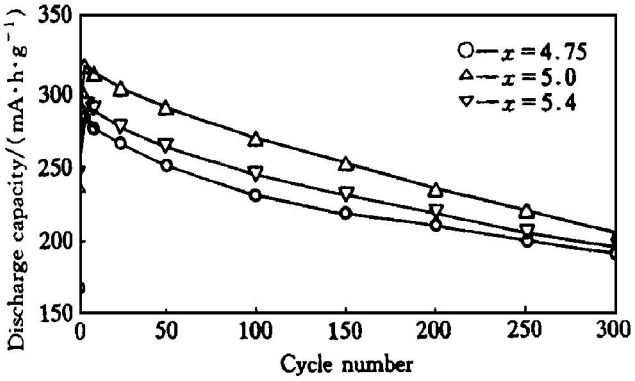

Fig. 4 Cycling curves of alloys $Ml(Ni_{0.82}Mn_{0.07}Al_{0.06}Fe_{0.05})_x$ ($4.75 \leqslant x \leqslant 5.4$)

bers. After 500 cycles, the discharge capacity attenuation rate (S_{500}) of AB_5 is 45.1%, that of $AB_{4.6}$ is only 30.3%, while that of $AB_{5.4}$ goes up to 48.9%. Because the crystalline sizes in a-axis and b-axis increase with increasing stoichiometry, and that in c-axis decreases with increasing stoichiometry (Table 1), It is believed that the decrease of the crystalline size in c-axis improves the pulverization resistance of the alloy due to their easily releasing micro-strain in c-axis during charge/discharge cycling, which results in better cycling stability for the over-stoichiometry alloys compared with the under-stoichiometric alloys.

Fig. 5 shows the discharge curves of the non-stoichiometric alloys for x = 4.75, 5.0 and 5.4 at the discharge rate of 50 mA·g^{-1}. It can be seen that the discharge potential of the alloys with higher stoichiometry is lower than that of the alloys with lower stoichiometry. The result indicates that stoichiometric alloy and over-stoichiometric alloys have even better discharge potential characteristics than the under-stoichiometric alloys.

The dependence of high-rate dischargeability on the discharge current density for the Ml(NiMnAlFe)$_x$ (x = 4.6, 5, 5.4) alloy electrodes is shown in Fig. 6. At the discharge rate of 300 mA·g^{-1}, the high-rate dischargeability of stoichiometry alloy ($AB_{5.0}$) reaches 87.2%, while the under-stoichiometric alloy $AB_{4.75}$ reaches 78.2%, that of the over-

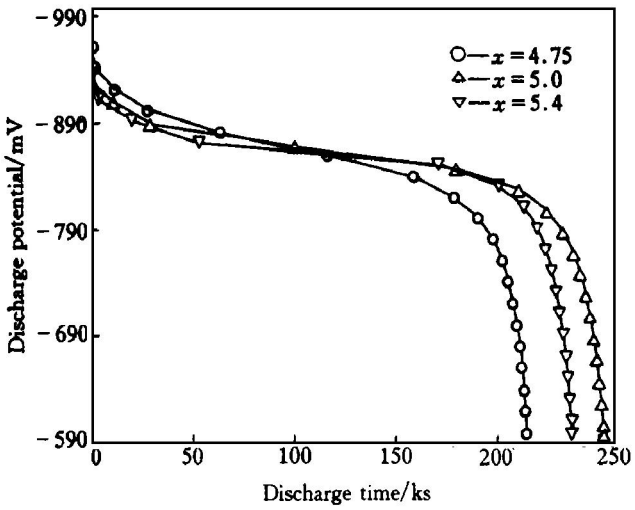

Fig. 5 Discharge potential curves of $Ml(Ni_{0.82}Mn_{0.07}Al_{0.06}Fe_{0.05})_x$

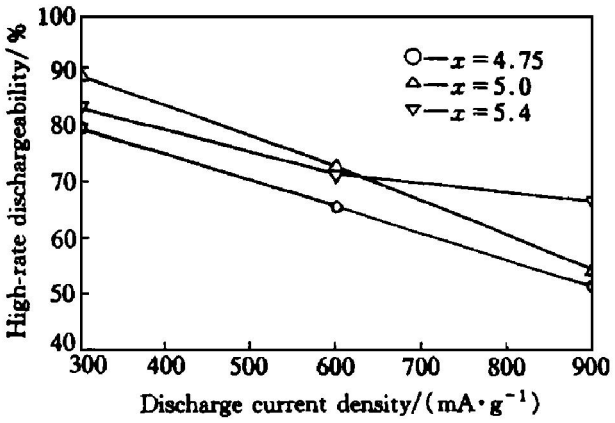

Fig. 6 High-rate dischargeability of alloys $Ml(Ni_{0.82}Mn_{0.07}Al_{0.06}Fe_{0.05})_x$

stoichiometry alloy $AB_{5.4}$ reaches 78.9%. At the discharge rate of 900 mA·g^{-1}, the high-rate dischargeability of the alloy $AB_{5.0}$ is 62.5%, that of $AB_{4.8}$ is 40.1% and $AB_{5.4}$ is 66.6%, respectively. This shows that the over-stoichiometric alloys ($x > 5.0$) have higher high-rate dischargeability and the under-stoichiometric alloys ($x < 5.0$) have lower high-rate dischargeability compared with the stoichiometric alloy (x = 5.0) in the $Ml(Ni_{0.82}Mn_{0.07}Al_{0.06}Fe_{0.05})_x$ alloys within 4.6~5.6. From XRD patterns, the alloys with $x \geqslant 5.0$ in Ml(NiMnAlFe)$_x$ have the secondary phase AlNi, which has good electrochemical catalytic property and can work as active sites on the surface of the electrode and to enhance the high-rate dischargeability of the alloy. The La-rich La_2Ni_7 and LaNi secondary phases, on the contrary, are proved to have a negative effect on high-rate dischargeability of the alloy.

4 CONCLUSIONS

The microstructure and electrochemical proper-

ties of non-stoichiometric Co-free Ml($Ni_{0.82}Mn_{0.07}Al_{0.06}Fe_{0.05}$)$_x$ ($4.6 \leqslant x \leqslant 5.6$) alloys were studied. It is found that the microstructure and electrochemical properties of the alloys are influenced greatly by stoichiometry. The alloys all have secondary phases besides the main $CaCu_5$ type structure phase with typical dendrite structure. The alloys have La_2Ni_7 and LaNi phases for $x \leqslant 5.0$, meanwhile the alloy have AlNi secondary phase for $x > 5.0$. The crystalline sizes in *a*-axis and *b*-axis increase with increasing stoichiometry, while the crystalline size in *c*-axis decreases with increasing stoichiometry. The stoichiometric alloy ($x = 5.0$) has the maximum discharge capacity ($C_{max} = 310\ mAh \cdot g^{-1}$), meanwhile the over-stoichiometric alloys ($x > 5.0$) have good high-rate dischargeability and cycling stability although their maximum discharge capacity lowered somewhat compared to the stoichiometric alloy ($x = 5.0$). The smaller crystalline sizes in *c*-axis is responsible for the improvement of the cycling stability of the over-stoichiometric alloys.

[REFERENCES]

[1] Willems J J G and Buschow K J H. From permanent magnets to rechargeable hydride electrodes [J]. J Less-Common Met, 1987, 129: 13.

[2] Kanda M, Yamamoto M, Kanno K, et al. Cyclic behaviour of metal hydride electrodes and the cell characteristics of nickel-metal hydride batteries [J]. J Less-Common Met, 1991, 172–174: 1227.

[3] Sakai T, Oguro K, Miyamura H, et al. Some factors affecting the cycle lives of $LaNi_5$-based alloy electrodes of hydrogen batteries [J]. J Less-Common Met, 1990, 161: 193.

[4] TANG W, GAI Y and ZHENG H. Deterioration of copper-containing mischmetal-nickel-based hydrogen absorption electrode materials [J]. J Alloys Comp, 1995, 224: 292.

[5] Hu W K, Kim D M, Tang K J, et al. Studies on Co-free rare-earth-based hydrogen storage alloys [J]. J Alloys Comp, 1998, 269: 254.

[6] Hu W K. Effect of microstructure, composition and non-stoichiometry on electrochemical properties of low-Co rare-earth nickel hydrogen storage alloys [J]. J Alloys Comp, 1998, 279: 295.

[7] Züttel A, Chartouni D, Gross K, et al. Relationship between composition, volume expansion and cyclic stability of AB_5-type metal hydride electrodes [J]. J Alloys Comp, 1997, 253–254: 626.

[8] Yasuda K. Effects of the materials processing on the hydrogen absorption properties of $MmNi_5$ type alloys [J]. J Alloys Comp, 1997, 253–254: 621.

[9] Notten P H L, Einerhand R E F and Daams J L C. On the nature of the electrochemical cycling stability of non-stoichiometric $LaNi_5$-based hydride-forming compounds Part I Crystallography and electrochemistry [J]. J Alloys Comp, 1994, 210: 221.

[10] Notten P H L, Einerhand R E F and Daams J L C. On the nature of the electrochemical cycling stability of non-stoichiometric $LaNi_5$-based hydride-forming compounds Part II In situ X-ray diffractometry [J]. J Alloys Comp, 1994, 210: 233.

[11] Higashiyama N, Matsuura Y, Nakamura H, et al. Influence of preparation methods of non-stoichiometric hydrogen-absorbing alloys on the performance of nickel-metal hydride secondary batteries [J]. J Alloys Comp, 1997, 253–254: 648.

[12] YANG Xiao-guang, LEI Yong-quan, CHEN Li-xin, et al. The electrochemical performances of Zr-based hydrogen storage alloys [J]. Trans Nonferrous Metal Soc China, 1995, 5(3): 61.

(Edited by HUANG Jin-song)